SUPPLEMENTAL INFORMATION

Therapeutic Disruption of RAD52-ssDNA Complexation via Novel Drug-Like Inhibitors

Divya S. Bhat [1], Eva Malacaria[2], Ludovica Di Biagi[2], Mortezaali Razzaghi[1], Masayoshi Honda[1], Kathryn F. Hobbs[1,3], Sarah R. Hengel[1,‡], Pietro Pichierri[2], M. Ashley Spies[1,3,*] and Maria Spies[1, *]

[1] Department of Biochemistry, University of Iowa Carver College of Medicine, 51 Newton Road, Iowa City, IA 52242, USA.

[2] Mechanisms, Biomarkers and Models section, Department of Environment and Health, Istituto Superiore di Sanità, Viale Regina Elena 299, 00161 Rome, Italy.

[3] Division of Medicinal and Natural Products Chemistry, Department of Pharmaceutical Sciences and Experimental Therapeutics, The University of Iowa, Iowa City, Iowa 52242, USA

[4] Naturis Informatika LLC., 401 Mullin Ave., Iowa City, Iowa 52246, USA

Supplemental Table S1. LC-MS analysis of the compounds used in this study

PLIF hits	
Z991573902	Chemical Formula: $C_{15}H_{11}N_3O_4$ MW: 297.3 Exact Mass: 297.075 RT: 5.8 min. $[M-H]^-$ at m/z 296.0675 (100%), 297.0709 (16.3%), 298.0735 (1.4%) $[M+H]^+$ at m/z 298.0820 (100%), 299.0854 (15.7%), 300.0882 (1.4%)
Z1347718341	Chemical Formula: $C_{13}H_{12}BrN_2O_5S$ MW: 388.2 Exact Mass: 386.9650 RT: 7.4 min. $[M]^-$ at m/z 388.9634 (100%), 386.9659 (97.2%), 389.9664 (14.7%) $[M+2H]^+$ at m/z 390.9774 (100%), 388.9796 (99.5%), 391.9806 (13.9%)
Z1633286133	Chemical Formula: $C_{17}H_{25}ClN_2O_2$ MW: 324.8 Exact Mass: 324.1605 RT: 3.1 min. $[M-H]^-$ at m/z 323.1534 (100%), 325.1505 (31.8%), 324.1569 (18.2%) $[M+H]^+$ at m/z 325.1676 (100%), 327.1644 (31.6%), 326.1705 (18.7%)
Docking/scoring function hits	
Z45684214	Chemical Formula: $C_{13}H_8F_2NO_5S$ MW: 328.3 Exact Mass: 328.0091 RT: 6.2 min. $[M]^-$ at m/z 328.0099 (100%), 329.0126 (15.1%), 330.0055 (4.0%)
Z56785913	Chemical Formula: $C_{15}H_{14}NO_5S$ MW: 320.3 Exact Mass: 320.0593 RT: 7.3 min. $[M]^-$ at m/z 320.0597 (100%), 321.0625 (16.9%), 322.0554 (4.3%) $[M+2H]^+$ at m/z 322.0739 (100%), 323.0774 (16.2%), 324.0697 (4.3%)
Z133609104	Chemical Formula: $C_{13}H_{10}NO_6S_2$ MW: 340.4 Exact Mass: 339.9950 RT: 6.5 min. $[M]^-$ at m/z 339.9953 (100%), 340.9979 (15.8%), 341.9908 (8.3%)
Z99 expansion compounds	
Z5862216254	Chemical Formula: $C_{15}H_9F_2N_3O_4$ MW: 333.2 Exact Mass: 333.2471 RT: 7.7 min. $[M-H]^-$ at m/z 332.0489 (100%), 333.0520 (16.0%), 334.0549 (1.6%) $[M+H]^+$ at m/z 334.0630 (100%), 335.0665 (15.2%), 336.0688 (1.4%)
Z586223162	Chemical Formula: $C_{15}H_9BrClN_3O_4$ MW: 410.6 Exact Mass: 408.9465 RT: 9.8 min. $[M-H]^-$ at m/z 409.9370 (100%), 407.9394 (78.0%), 411.9341 (24.2%)
Z586214869	Chemical Formula: $C_{16}H_{12}BrN_3O_4$ MW: 390.2 Exact Mass: 389.0011 RT: 9.6 min. $[M-H]^-$ at m/z 387.9943 (100%), 389.9923 (98.9%), 388.9978 (17.3%)
Z586220972	Chemical Formula: $C_{16}H_{12}ClN_3O_4$ MW: 345.7 Exact Mass: 345.0516 RT: 9.4 min. $[M-H]^-$ at m/z 344.0449 (100%), 346.0417 (31.4%), 345.0482 (17.4%) $[M+H]^+$ at m/z 346.0590 (100%), 348.0559 (29.4%), 347.0625 (16.0%)
Z586213583	Chemical Formula: $C_{16}H_{12}FN_3O_4$ MW: 329.3 Exact Mass: 329.0812 RT: 7.9 min. $[M-H]^-$ at m/z 328.0742 (100%), 329.0774 (17.1%), 330.0802 (1.8%) $[M+H]^+$ at m/z 330.0884 (100%), 331.0918 (16.8%), 332.0946 (1.6%)

Supplemental Table S2. Media components for all cell lines used in this study

Cell line	Media components
MCF10a (BRCA-positive)	DMEM/F12 (Gibco/ThermoFisher Scientific, Waltham, MA, USA), 5% Horse serum (Invitrogen Waltham, MA, USA), 20ng/mL EGF (Peprotech, Rocky Hill, NJ, USA), 0.5mg/mL Hydrocortisone (Sigma-Aldrich, *Saint Louis, MO, USA),* 100ng/mL Cholera toxin (Sigma-Aldrich, *Saint Louis, MO, USA)*, 10μg/mL Insulin (Sigma-Aldrich, *Saint Louis, MO, USA)*, 100U/mL Pen/Strep (Gibco/ThermoFisher Scientific, Waltham, MA, USA).
MRC5SV40	DMEM low-glucose (Gibco/ThermoFisher Scientific, Waltham, MA, USA) supplemented with 10% FBS and 2mM L-Glutamine
MRC5SV40shRAD52	DMEM low-glucose (Gibco/ThermoFisher Scientific, Waltham, MA, USA) supplemented with 10% FBS and 2mM L-Glutamine, 500ng/ml puromycin
EUFA423F (7691 insAT in allele 1, and 9900 insA in allele 2 of *BRCA2*)	DMEM, 10% FBS, 20mM HEPES, 100U/mL Pen/Strep (all from Gibco/ThermoFisher Scientific, Waltham, MA, USA).
EUFA423F –HA (BRCA2-complemented)	DMEM, 10% FBS, 20mM HEPES, 100U/mL Pen/Strep (all from Gibco/ThermoFisher Scientific, Waltham, MA, USA), 500μg/mL G418 (IBI Science, Dubuque, IA, USA).
Capan 1	IMDM, 15% FBS (Gibco/ThermoFisher Scientific, Waltham, MA, USA), 2mM L-Glutamine, 100U/mL Pen/Strep (all from Gibco/ThermoFisher Scientific, Waltham, MA, USA).
MDA-MB 436	DMEM [Cat# 11960-069] ,10% FBS, 1mM sodium pyruvate, 10mM non-essential amino acids, 100U/mL Pen/Strep and 2mM GlutaMax (all from Gibco/ThermoFisher Scientific, Waltham, MA, USA).

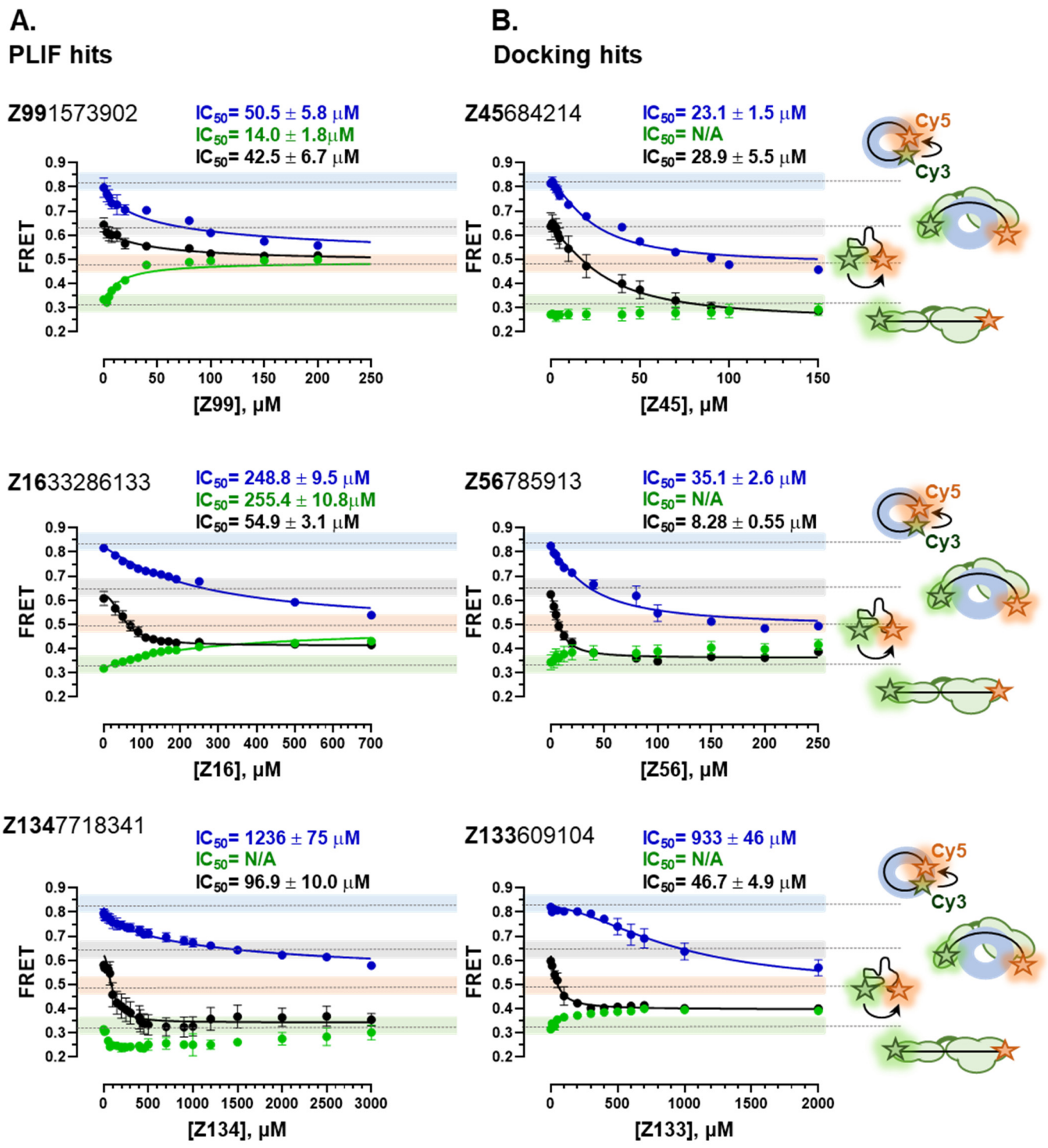

Supplemental Figure S1. **All six novel compounds inhibit the RAD52-ssDNA interactions**. The *in vitro* FRET-based assays follow inhibition of the RAD52-ssDNA interaction (blue circles and lines), RPA-ssDNA interactions (green circles and lines), and the interaction between RAD52 and RPA-ssDNA complex (black circles and lines). The identity of each compound is indicated above the respective graphs. Complexes at the starting point of inhibitor titrations are depicted schematically on the right. The data shown as average ± standard deviation for at least three independent measurements. Where invisible, the error bars are smaller than the respective symbols. Calculated IC_{50} values are shown above each graph.

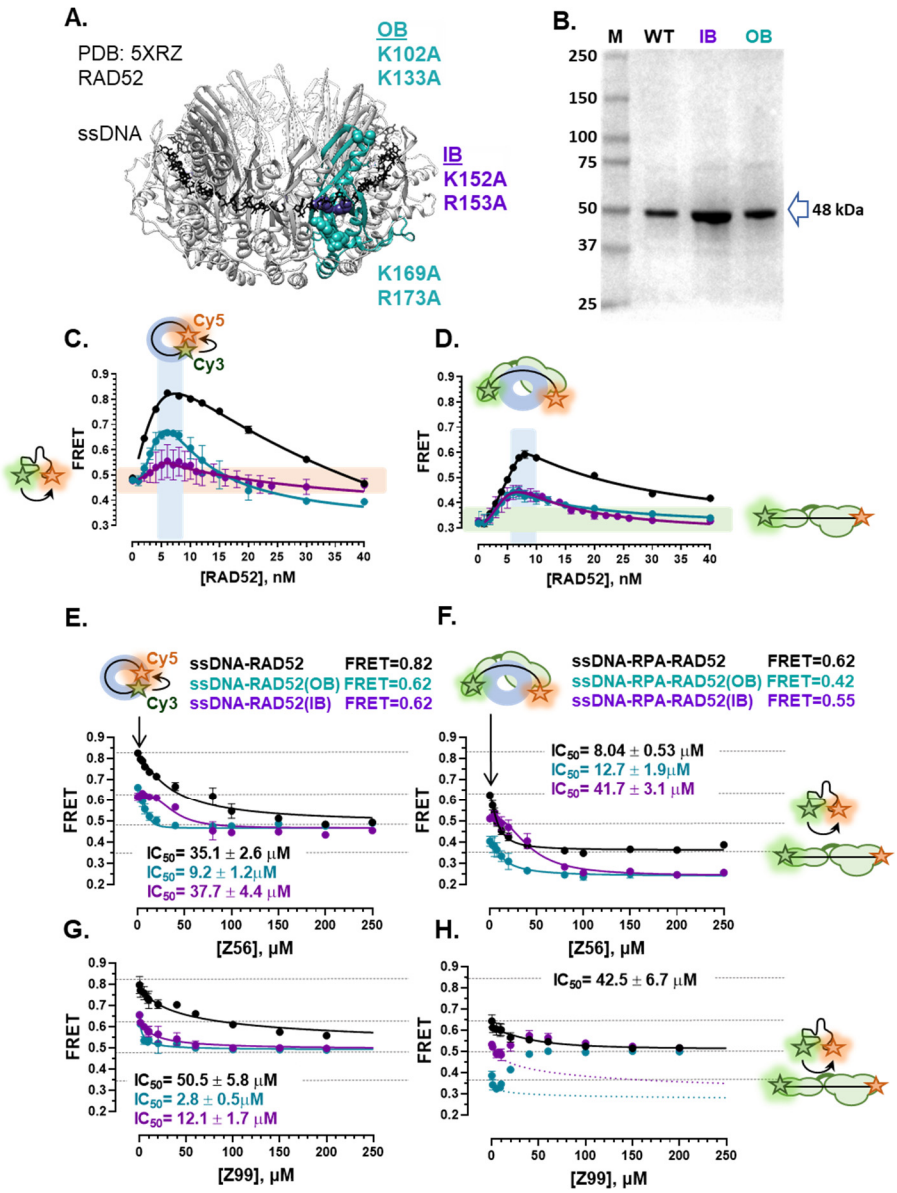

Supplemental Figure S2. **Effect of the Z56 and Z99 compounds on the RAD52 mutants with defects in the two DNA binding regions. A.** Residues in the inner (purple, IB) and outer (teal, OB) DNA binding sites are mapped on the crystal structure of the RAD52-ssDNA complex (PDB: 5XRZ). These residues were substituted with alanines resulting outer binding deficient mutant (OB) and inner binding deficient mutant (IB), respectively. **B**. SDS-PAGE gel showing the wild type and mutant RAD52 proteins. **C**. Binding of the wild type (black), IB (purple) and OB (teal) RAD52 to 1 nM Cy3/Cy5 labeled dT30 ssDNA yield binding isotherms with the same characteristic shape suggesting two DNA binding modes, the ssDNA fully wrapped around the RAD52 ring (High FRET) and the ssDNA shared between multiple rings. The blue bar behind the graph highlights the concentration range where the FRET of the ssDNA complex is the most different from that of the free ssDNA (the pink horizontal bar behind the graph). **D**. The same as (**C**), except the RPA-ssDNA complex was used as a substrate for RAD52 binding. The low FRET values of the "wrapped" complex observed for both mutants indicates either smaller distortion of the DNA within the complex, or more similar affinities of the two binding modes. **E-H**. Inhibition of the wild type and mutant RAD52 with small molecules highlights the importance of both DNA binding sites. Inhibition of the RAD52 (wild type or mutant) interaction with ssDNA by Z56 (**E**) and Z99 (**G**). Both inhibitors were more effective against the RAD52-OB mutants, which correlates well with the placement of this inhibitors in the DNA binding grove. In contrast, activity of Z56 was reduced when targeting the RAD52 mutants bound to RPA-coated ssDNA (**F**). Similar to the wild type RAD52-RPA-ssDNA complex, Z99 removed both RAD52 mutants and RPA from ssDNA (**H**).

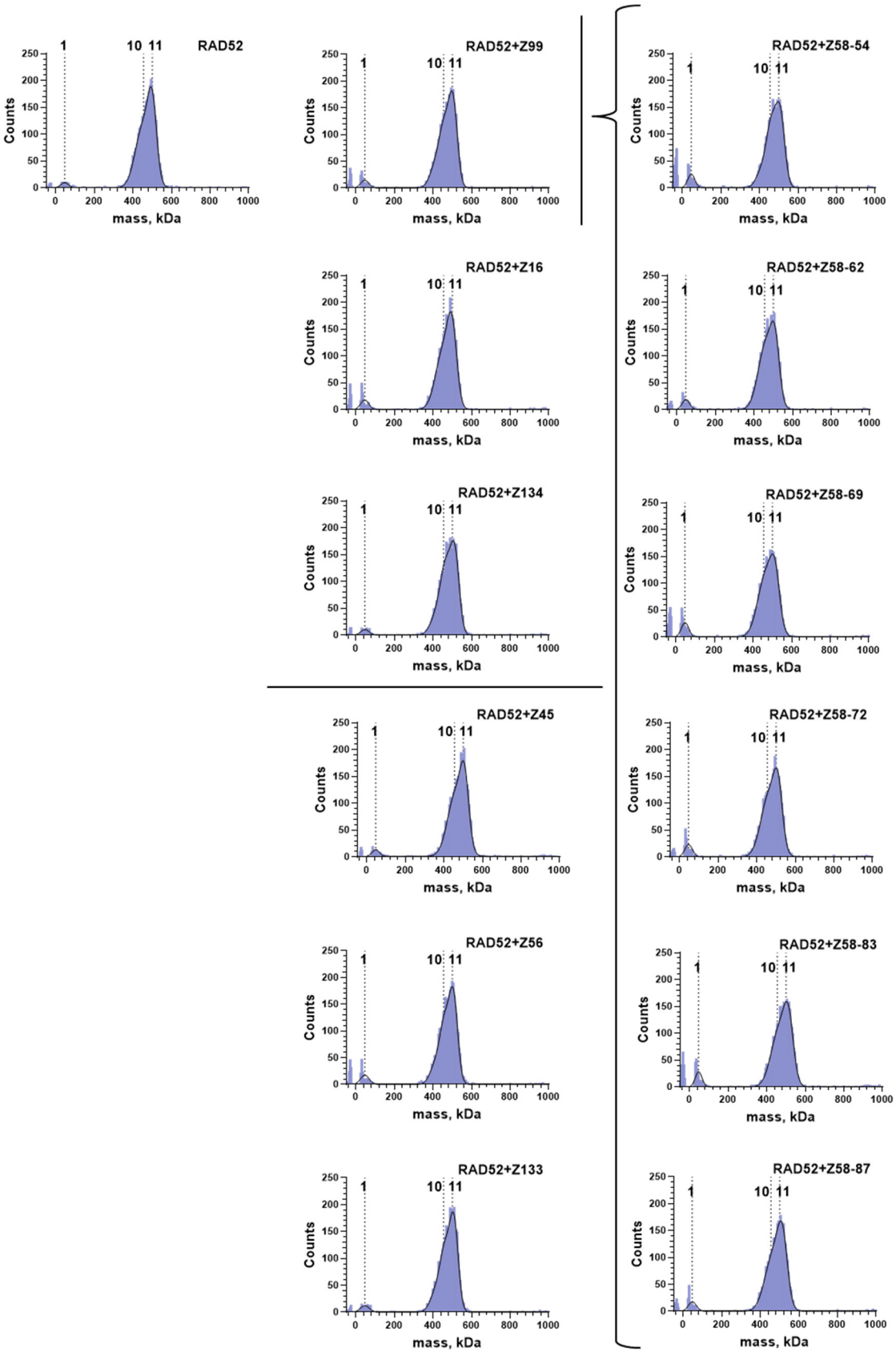

Supplemental Figure S3. **None of the synthesized compounds disrupt the RAD52 oligomer.** Mass Photometry analysis of the RAD52 protein (100 nM final concentration) in the presence or absence of 50 μM of respective inhibitors. The histograms show the masses of the molecules in solution binned into 5 kDa bins and plotted as histograms (blue). The binned data were than fitted to a sum of three or four Gaussians (black line). Dotted lines indicate locations of the centers of the monomer, decamer and undecamer peaks.

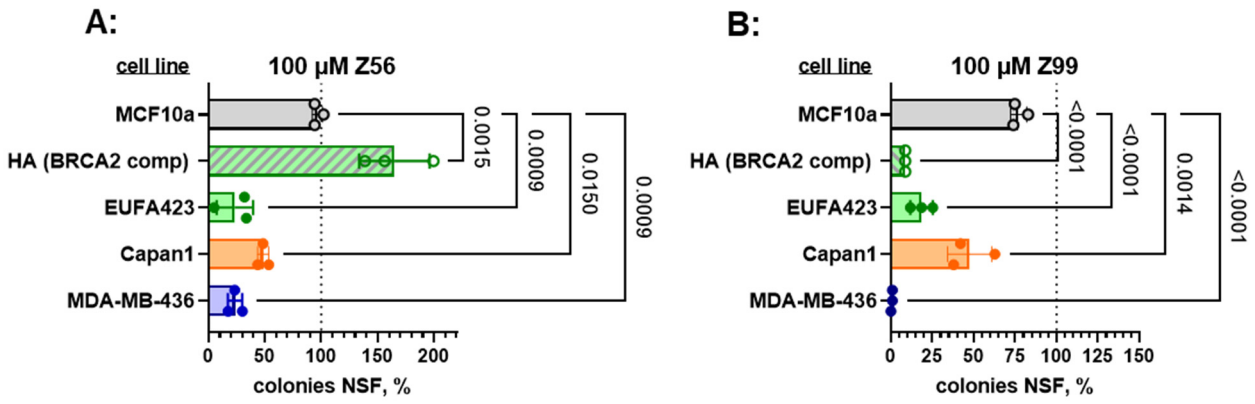

Supplemental Figure S4. **Z56 and Z99 interfere with the ability of BRCA-deficient cells to produce colonies.** Colony formation was measured for the indicated cell lines after 72hrs treatment with 100 µM of Z56 (**A**) or Z99 (**B**). The data are shown as individual measurements along with average ± standard deviation for 3 independent plates. Colonies were quantified and normalized for average number of colonies observed after DMSO only treatment for each cell line. Statistical pairwise comparisons were carried out using Ordinary ANOVA in GraphPad Prism.

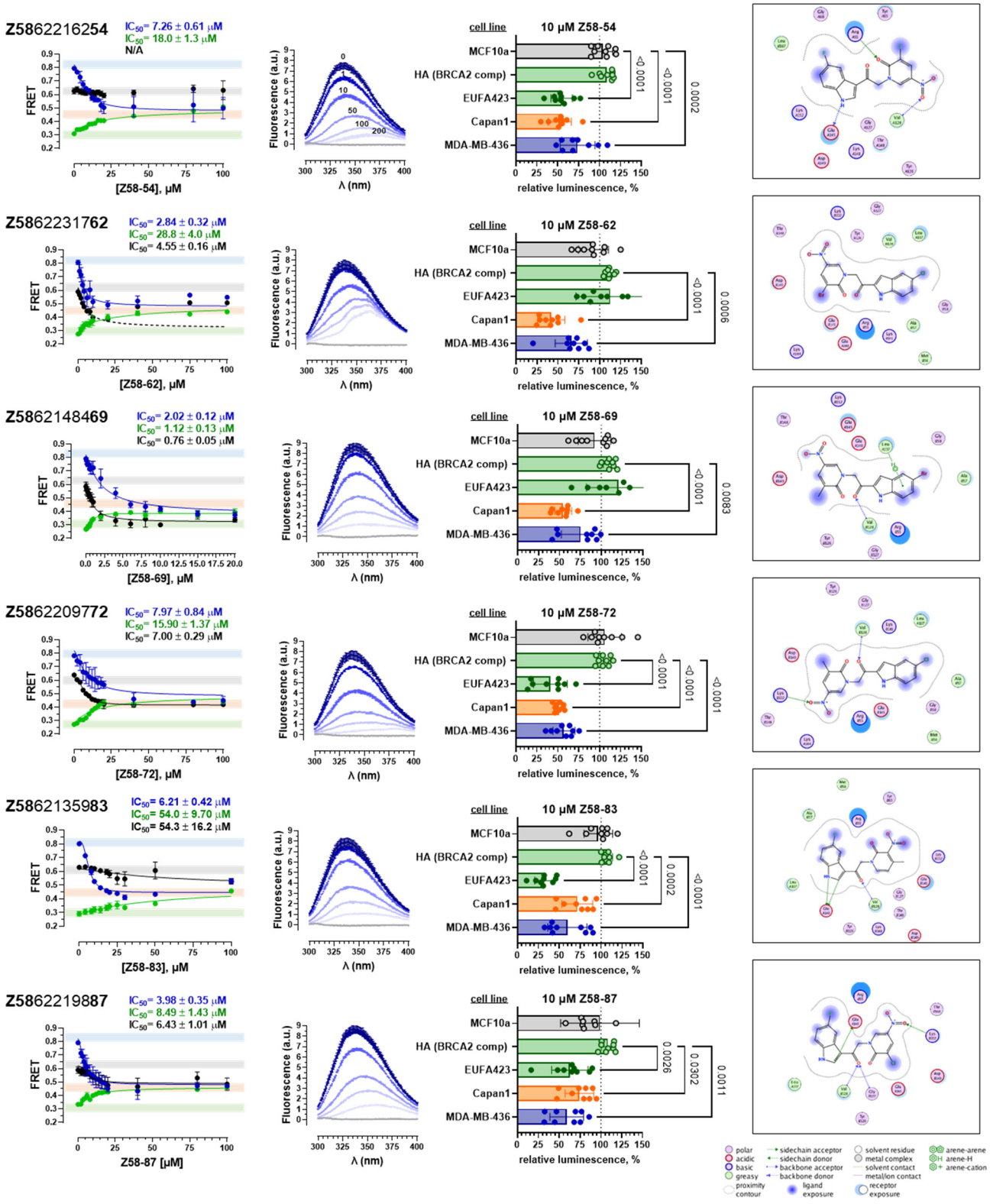

Supplemental Figure S5. Detailed analysis of the Z99 scaffold expansion compounds. For each compound, the graphs of the FRET based experiments along with calculated IC_{50} values are shown in the left panel (blue – inhibition of the RAD52-ssDNA complex, green – inhibition of the RPA-ssDNA complex, and black – inhibition of the RPA-ssDNA-RAD52 complex). The second from the left panels show intrinsic tyrosine fluorescence experiments that follow direct binding of each compound to RAD52. The third from the left panels show viability experiments using CellTiter-Glo® luminescence assay. The data are shown as individual measurements along with average ± standard deviation for 9 independent measurements. The response of each cell lines was compared to MCF10a (ns = not significant P>0.05; *P<0.05; **P<0.01; ***P<0.001; ****P < 0.0001; Ordinary ANOVA). The right panels show the ligand maps.

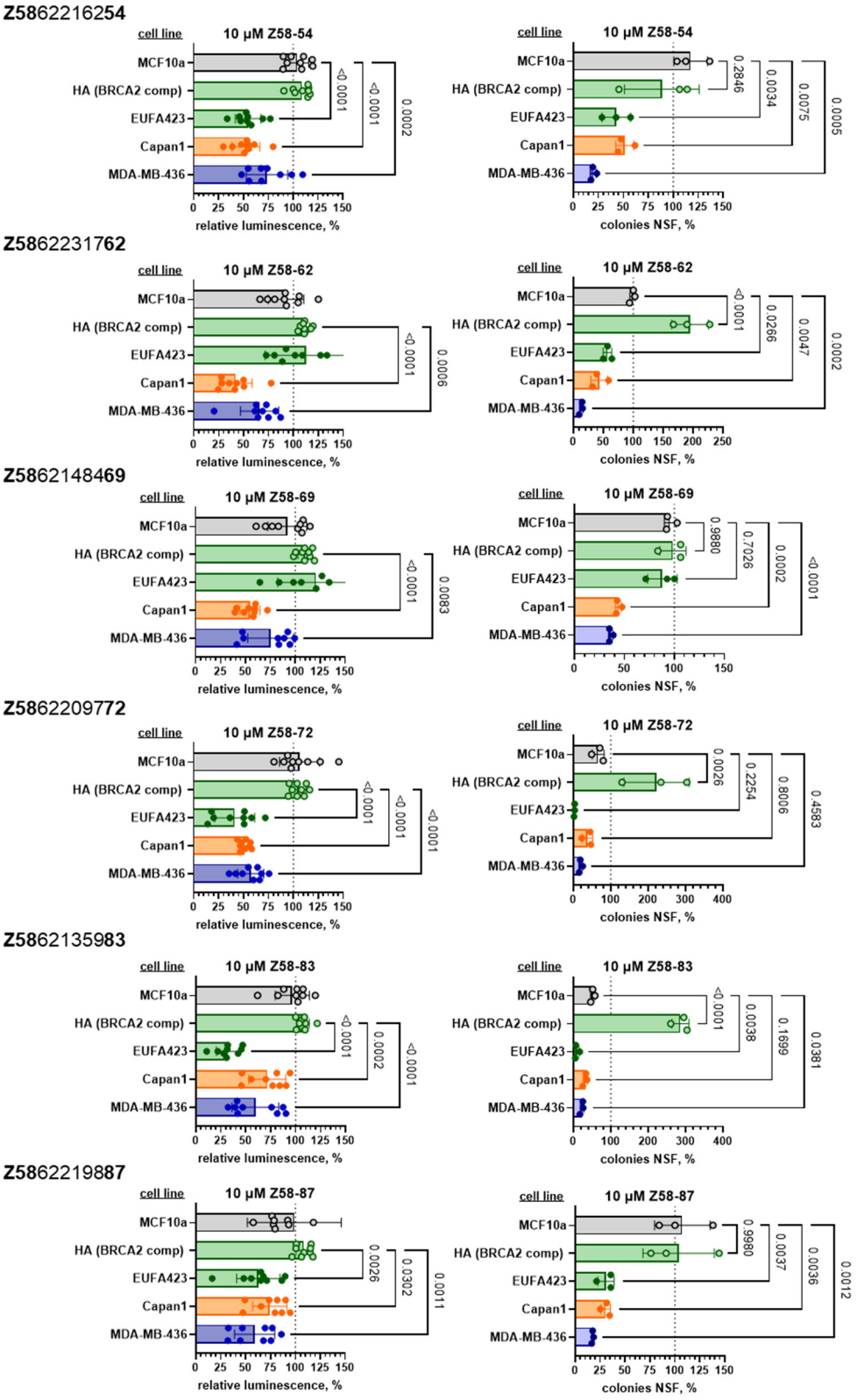

Supplemental Figure S6. Viability and colony formation by the Z99 scaffold expansion compounds. Viability experiments using CellTiter-Glo® luminescence assay (left panels) are compared to clonigenic potential (right panels) for all compounds. CellTiter-Glo® luminescence data are shown as individual measurements along with average ± standard deviation for 9 independent measurements. Colony formation was measured for 5 cell lines after 72hrs treatment with 10 µM of indicated compound. The data are shown as individual measurements along with average ± standard deviation for 3 independent plates. Colonies were quantified and normalized for average number of colonies observed after DMSO only treatment for each cell line. The response of each cell lines was compared to MCF10a using Ordinary ANOVA.

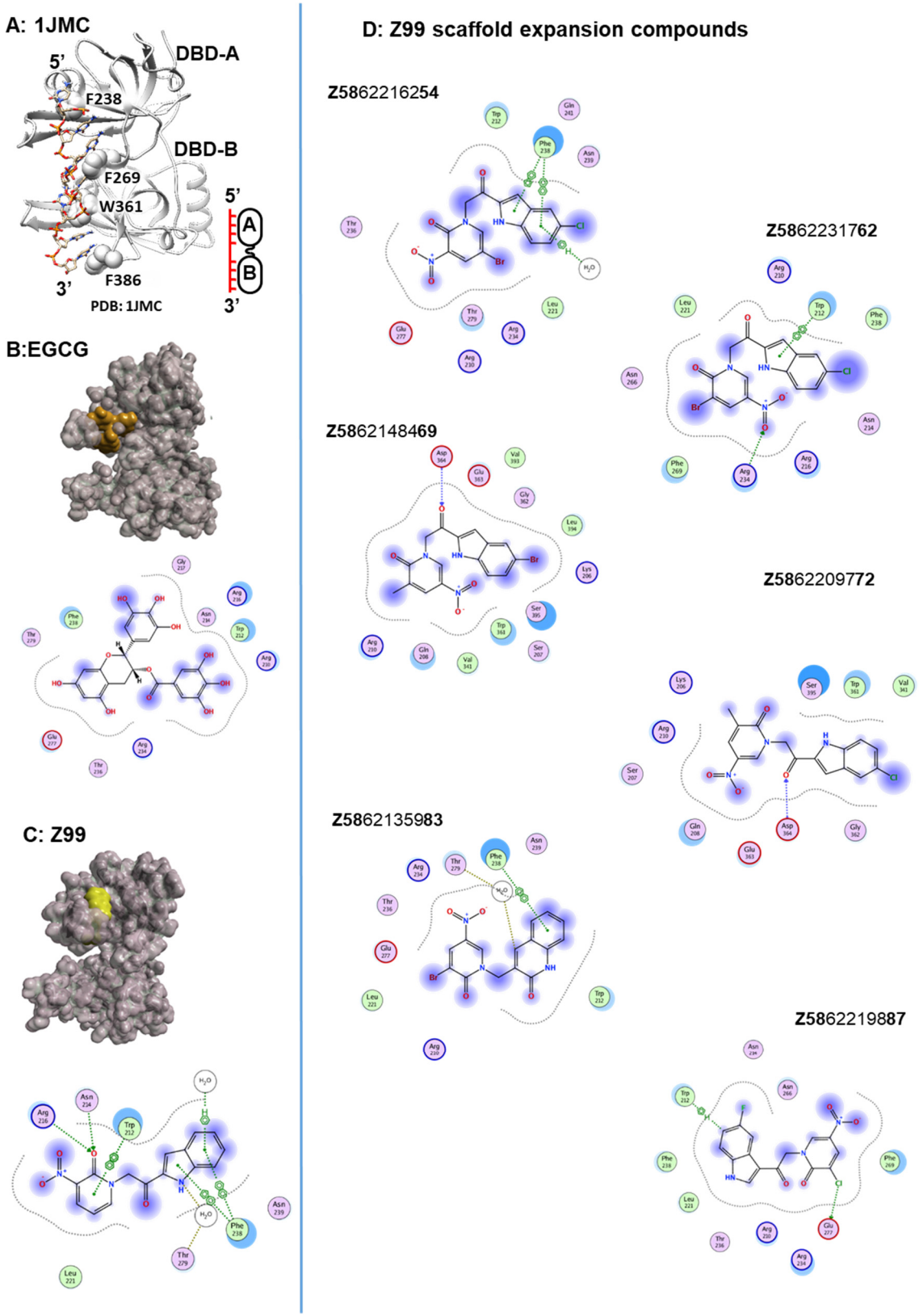

Supplemental Figure S7. **Compounds that promiscuously inhibit both the RAD52- and the RPA-ssDNA interaction reside in the ssDNA binding site of RPA DBD-A**. **A**. Ribbon diagram and cartoon representation of the DBD-A/B of human RPA (PDB:1JMC). The key aromatic residues in the ssDNA binding site are shown as spheres. **B&C**. surface representation and ligand maps for EGCG and Z99 best docking poses. **B**. The best docking pose for EGCG places this natural product into the ssDNA binding site of DBD-A with an additional stacking interaction to W212. **C**. The best docking pose for the Z99 compound partially overlaps with that of EGCG and displays many of the same contacts. **D**. Ligand maps for the Z99 scaffold expansion compounds.

Molecule 1

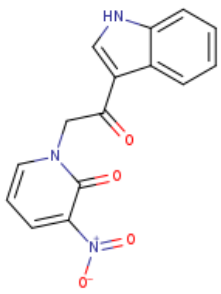

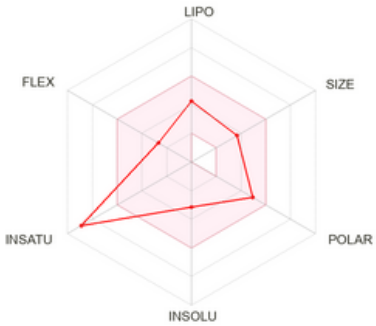

SMILES O=C(c1c[nH]c2c1cccc2)Cn1cccc(c1=O)[N+](=O)[O-]

Physicochemical Properties	
Formula	C15H11N3O4
Molecular weight	297.27 g/mol
Num. heavy atoms	22
Num. arom. heavy atoms	15
Fraction Csp3	0.07
Num. rotatable bonds	4
Num. H-bond acceptors	4
Num. H-bond donors	1
Molar Refractivity	82.36
TPSA	100.68 Å²

Lipophilicity	
Log $P_{o/w}$ (iLOGP)	0.88
Log $P_{o/w}$ (XLOGP3)	1.97
Log $P_{o/w}$ (WLOGP)	2.12
Log $P_{o/w}$ (MLOGP)	1.17
Log $P_{o/w}$ (SILICOS-IT)	0.68
Consensus Log $P_{o/w}$	1.36

Water Solubility	
Log *S* (ESOL)	-3.16
Solubility	2.03e-01 mg/ml ; 6.84e-04 mol/l
Class	Soluble
Log *S* (Ali)	-3.71
Solubility	5.80e-02 mg/ml ; 1.95e-04 mol/l
Class	Soluble
Log *S* (SILICOS-IT)	-4.23
Solubility	1.73e-02 mg/ml ; 5.83e-05 mol/l
Class	Moderately soluble

Pharmacokinetics	
GI absorption	High
BBB permeant	No
P-gp substrate	No
CYP1A2 inhibitor	Yes
CYP2C19 inhibitor	No
CYP2C9 inhibitor	No
CYP2D6 inhibitor	No
CYP3A4 inhibitor	No
Log K_p (skin permeation)	-6.71 cm/s

Druglikeness	
Lipinski	Yes; 0 violation
Ghose	Yes
Veber	Yes
Egan	Yes
Muegge	Yes
Bioavailability Score	0.55

Medicinal Chemistry	
PAINS	0 alert
Brenk	2 alerts: nitro_group, oxygen-nitrogen_single_bond
Leadlikeness	Yes
Synthetic accessibility	2.43

Supplemental Figure S8. ADME properties of Z99

Molecule 1

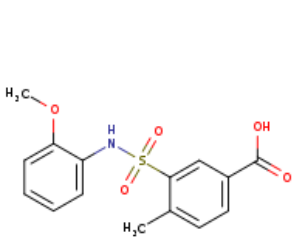

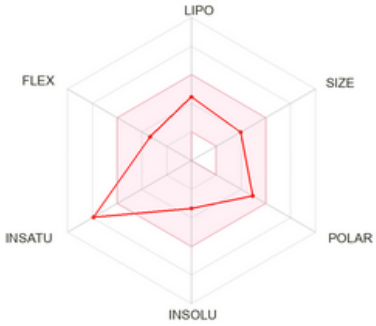

SMILES COc1ccccc1NS(=O)(=O)c1cc(ccc1C)C(=O)O

Physicochemical Properties	
Formula	C15H15NO5S
Molecular weight	321.35 g/mol
Num. heavy atoms	22
Num. arom. heavy atoms	12
Fraction Csp3	0.13
Num. rotatable bonds	5
Num. H-bond acceptors	5
Num. H-bond donors	2
Molar Refractivity	81.97
TPSA	101.08 Å²

Lipophilicity	
Log $P_{o/w}$ (iLOGP)	1.67
Log $P_{o/w}$ (XLOGP3)	2.31
Log $P_{o/w}$ (WLOGP)	3.39
Log $P_{o/w}$ (MLOGP)	1.76
Log $P_{o/w}$ (SILICOS-IT)	1.48
Consensus Log $P_{o/w}$	2.12

Water Solubility	
Log *S* (ESOL)	-3.36
Solubility	1.40e-01 mg/ml ; 4.35e-04 mol/l
Class	Soluble
Log *S* (Ali)	-4.07
Solubility	2.73e-02 mg/ml ; 8.49e-05 mol/l
Class	Moderately soluble
Log *S* (SILICOS-IT)	-4.76
Solubility	5.61e-03 mg/ml ; 1.75e-05 mol/l
Class	Moderately soluble

Pharmacokinetics	
GI absorption	High
BBB permeant	No
P-gp substrate	No
CYP1A2 inhibitor	No
CYP2C19 inhibitor	No
CYP2C9 inhibitor	Yes
CYP2D6 inhibitor	No
CYP3A4 inhibitor	No
Log K_p (skin permeation)	-6.62 cm/s

Druglikeness	
Lipinski	Yes; 0 violation
Ghose	Yes
Veber	Yes
Egan	Yes
Muegge	Yes
Bioavailability Score	0.56

Medicinal Chemistry	
PAINS	0 alert
Brenk	0 alert
Leadlikeness	Yes
Synthetic accessibility	2.62

Supplemental Figure S9. ADME properties of Z56